Department of the Navy
Office of Naval Research
Contract N6onr-24435

MEASUREMENT OF DYNAMIC COEFFICIENTS OF ELLIPSOIDS

John A. Stallkamp

Hydrodynamics Laboratory
California Institute of Technology
Pasadena, California

Report No. E-35.4

September 1956

Department of the Navy
Office of Naval Research
Contract N6onr-24435

MEASUREMENT OF DYNAMIC COEFFICIENTS OF ELLIPSOIDS

John A. Stallkamp

Hydrodynamics Laboratory
California Institute of Technology
Pasadena, California

Report No. E-35.4 September 1956

ABSTRACT

The measurement of dynamic coefficients in a water tunnel is considered generally, and it is shown that the forces depend only on relative velocity provided the flow in the water tunnel is steady. A method of measuring the coefficient N_r, relating cross force to yawing angular velocity utilizing an internal balance, is described. Experimental results are compared with theory, showing good agreement in the case of the coefficient N_r.

CONTENTS

MOTION IN A PERFECT FLUID

The method of solution of the problem of the motion of a rigid body in an infinite volume of frictionless incompressible fluid is well known. It consists in demonstrating that for the purpose of obtaining the fluid reactions on the body, the fluid may be removed and its effect replaced or represented by quantities analogous to inertias. These quantities are often called the assessed or virtual masses and moments of inertia and the cross-products of inertia. They are all, in general, directionally dependent, that is, they are functions of the orientation of the body with respect to its motion. The motion of this composite rigid body, consisting of the original body and the several virtual inertia quantities, is then examined. Generalized forms and methods of dynamics of a rigid body in free space are used when necessary. For example, the linear kinetic energy may no longer be proportional to the square of the total linear velocity but may now be a generalized quadratic form in all of the components of the linear velocity.

The hydrodynamic reactions on the body can then be computed from the motion of the body. For the two-dimensional motion of a prolate ellipsoidal body in the plane of yaw in a perfect fluid the equations are:

$$X = - M_o k_1 \dot{u} + M_o k_2 v r \tag{1}$$

$$Y = - M_o k_2 \dot{v} - M_o k_1 u r \tag{2}$$

$$N = - I_o k' \dot{r} - M_o (k_2 - k_1) u v . \tag{3}$$

These perfect fluid coefficients may be identified with the force and moment derivatives of the standard nomenclature.

$$M_o k_1 = - X_{\dot{u}} \tag{4}$$

$$M_o k_2 = - Y_{\dot{v}} \qquad \text{perfect fluid coefficients} \tag{5}$$

$$I_o k' = - N_{\dot{r}} \tag{6}$$

The reader is referred to Milne-Thomson's "Theoretical Hydrodynamics" or Lamb's "Hydrodynamics" for a rigorous derivation of equations (1), (2), and (3).

For motion in a real fluid, the viscosity of the fluid can become the sole factor in determining the fluid reactions on the body; however, the magnitudes of the viscous effects are usually functions of Reynolds number. For the body shape and the ranges of body sizes and of tunnel velocities encountered in the present experimental work, they are important but do not overshadow the perfect fluid reactions.

Since the experimental work was performed in a water tunnel, some questions arise regarding the applicability of an analytic perfect fluid solution (where the fluid motion at a large distance from the body is taken to be zero) to the present case for the same relative velocity between the tunnel water and the ellipsoidal model. In the texts cited, zero fluid velocity at infinity is assumed and this assumption is used in an explicit manner in the solutions that lead to the virtual inertia terms. For this case the natural choice of the inertial frame of reference is this zero velocity field; all motions of the body and fluid and the associated forces and moments are defined with respect to this frame. If measurements are made in a second inertial system and if from these measurements the reactions in the first system are to be inferred, the solutions to both situations must be known. For the invariant scalar inertia of particles and rigid bodies, the necessary relationships are known immediately from Newtonian mechanics. As shown in references 1 and 2, however, it is only for the condition of zero fluid motion at infinity that the fluid reactions on the body can be evaluated from the reactions on suitable inertial type quantities. That these same virtual inertia terms are applicable directly in other inertial systems is not proved and indeed is not true. The case of the two-dimensional motion of a prolate ellipsoid is given in Appendix II. Zero angular motion of the fluid at a distance is assumed throughout. It is shown that only for zero acceleration of the fluid at a distance will the perfect fluid reactions on the body be functions of the relative motion of the body and fluid. Thus, the perfect fluid reactions measured in a constant velocity water tunnel for any motion of the body relative to the tunnel will be identical to the fluid reactions in a volume of fluid at rest at a great distance from the body when the relative motions of the body and fluid are the same. It is, of course, recognized that tunnel wall effects have not been considered here.

EXPERIMENTAL PROGRAM

The broad objective of the experimental program is the measurement of damping and inertial or acceleration hydrodynamic reactions on totally wetted prolate ellipsoidal-shaped bodies. The reactions to be measured are the lateral forces and yawing moments proportional to angular velocity and acceleration for the body translating at constant linear velocity and oscillating through a small angle of yaw. Linearization as a result of restriction to small amplitude of angle of yaw is assumed. Precise specification of the motion of the body and of the linearization is given. Particular emphasis is placed on the measurement of the component of lateral force due to angular velocity.

The measurement equipment is described in detail. In the experimental work the body is mounted in a water tunnel and oscillated sinusoidally about the zero angle of yaw position by means of a torsion spring. The moment reaction is determined in an indirect manner; that is, the response amplitude and phase angle of the forced oscillation are measured and the components of moment are calculated from the dynamic equations of the system. The total instantaneous lateral force is measured directly by means of a spring balance located inside the body and its several components are then evaluated.

Hydrodynamics of the Experimental Program

Experimental tests were made to determine the fluid damping and dynamic or inertial forces and moments on a series of prolate ellipsoidal bodies for small angle of yaw, constant linear velocity motion in water. The geometric center of the ellipsoid is fixed in the working section of the tunnel. The body is oscillated with small amplitude about a mean position in which its long axis coincides with the direction of flow of the water.

The angular motion is restricted to the horizontal or yaw plane; its analytic description is given by the following equations:

U	constant relative linear velocity of the origin of body and fluid at a distance.
$\beta = \beta(t)$	angle of drift or angle of yaw for zero roll.

$u = U \cos \beta$ components of the relative linear velocity of the body

$v = -U \sin \beta$ and fluid at a distance resolved along body axes.

$r = \dot{\beta}$ angular velocity of body.

Although it is normally used for the angle of drift, the symbol β will be used for the angle of yaw in this report. This is not a violation of the standard nomenclature since the angles of drift and yaw are identical for this two-dimensional motion of the body in the fluid.

The hydrodynamic yawing moment and lateral force are assumed to be linear functions of the yaw angle and its first and second derivatives for the small angles through which the model is permitted to move.

$$Y = -m\ddot{\beta} + b\dot{\beta} + k\beta \tag{7}$$

$$N = -I_f \ddot{\beta} - B\dot{\beta} - K\beta \tag{8}$$

The nomenclature for the six coefficients in the above equations has been chosen to facilitate the writing of subsequent equations. These terms are, in fact, various combinations of the usual hydrodynamic force and moment derivatives. This will now be shown. Since the angle of yaw, β, is small the simplification $\sin \beta = \beta$ and $\cos \beta = 1$ is applicable.

$$\begin{aligned} u &= U \cos \beta = U \\ v &= U \sin \beta = -U\beta \\ \dot{v} &= U \cos \beta\dot{\beta} = -U\dot{\beta} \end{aligned} \tag{9}$$

From the symmetry of the body Y_u, $Y_{\dot{u}}$, $N_{\dot{u}}$, and N_u are zero.

$$\begin{aligned} Y &= Y_{\dot{v}}\dot{v} + Y_v v + Y_{\dot{r}}\dot{r} + Y_r r \\ &= Y_{\dot{r}}\ddot{\beta} + (Y_r - Y_{\dot{v}} U)\dot{\beta} - Y_v U\beta \end{aligned} \tag{10}$$

$$\begin{aligned} N &= N_{\dot{r}}\dot{r} + N_r r + N_{\dot{v}}\dot{v} + N_v v \\ &= N_{\dot{r}}\ddot{\beta} + (N_r - N_{\dot{v}} U)\dot{\beta} - N_v U\beta \ . \end{aligned} \tag{11}$$

Term by term identification between equations (7), (8), (10) and (11) is now made.

$$\begin{aligned} m &= Y_{\dot{r}} \quad b = (Y_r - Y_{\dot{v}} U) \quad k = -Y_v U \\ I_f &= -N_{\dot{r}} \quad B = -(N_r - N_{\dot{v}} U) \quad K = N_v U \ . \end{aligned} \tag{12}$$

For comparison, the equations for the hydrodynamic reactions for the same motion of the ellipsoidal body and fluid but in a perfect fluid are given here. They are taken from Appendix II.

$$Y = M_o(k_2 - k_1)\, U\dot{\beta} \tag{13}$$

$$N = I_o k'\ddot{\beta} + M_o(k_2 - k_1)\, U^2\beta . \tag{14}$$

Experimental Method

The experimental measurements were made in the High Speed Water Tunnel at the California Institute of Technology using small amplitude, steady-state, forced sinusoidal oscillations. The measurement of the fluid reactions is facilitated by the stationary character of the steady-state motion. The random transient reactions present in the motion of a real fluid are averaged out over many cycles of motion. Further discussion of this is given after the individual descriptions of the moment and force-measuring systems.

The equations of motion of the body-fluid system are now formulated. The center of gravity of the test body is at the center or axis of support and rotation. Therefore, its only dynamic reaction is a torque due to angular acceleration.

$$\beta = A_o \sin(\omega t - \delta_o) \quad \text{angular motion of body.} \tag{15}$$

$$Y_s = -Y = m\ddot{\beta} - b\dot{\beta} - k\beta = \text{lateral force on body in fluid supplied by the support, along instantaneous position of y body axis.} \tag{16}$$

$$N_s = I_b\ddot{\beta} - N = (I_b + I_f)\ddot{\beta} + B\dot{\beta} + K\beta \tag{17}$$

$$= I\ddot{\beta} + B\dot{\beta} + K\beta$$

$$= \text{Yawing moment on body in fluid supplied by support.}$$

(a) Measurement of Moment

Pictures of the balance installed in the High Speed Water Tunnel are given in Figs. 1 and 2. A schematic diagram of its operation is given in Fig. 3.

The test model is secured to a vertical spindle carried in ball-bearings in the balance structure. The space between the spindle and the tunnel wall

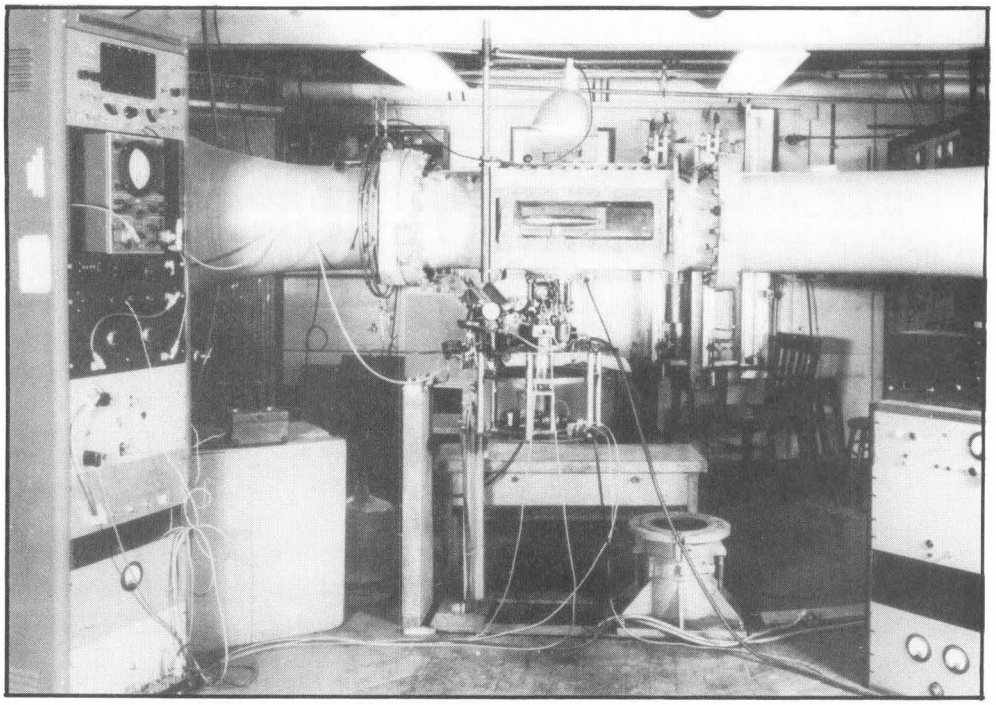

Fig. 1 - Dynamic balance in place in the working section of the High Speed Water Tunnel and its electronic instrumentation.

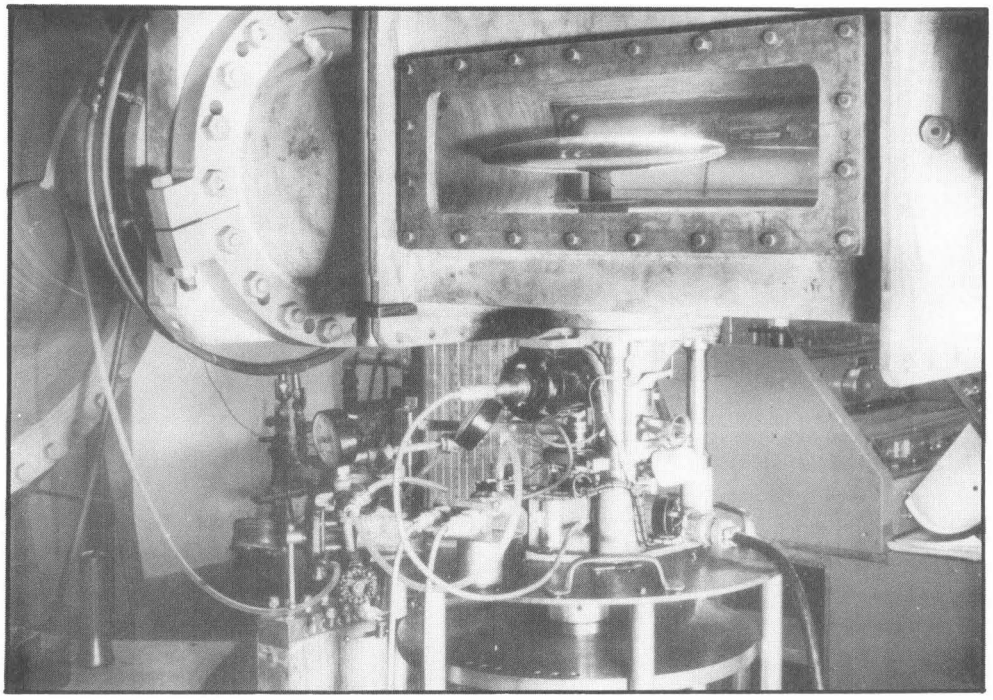

Fig. 2 - Close-up photograph of the elliptical model in the working section of the High Speed Water Tunnel.

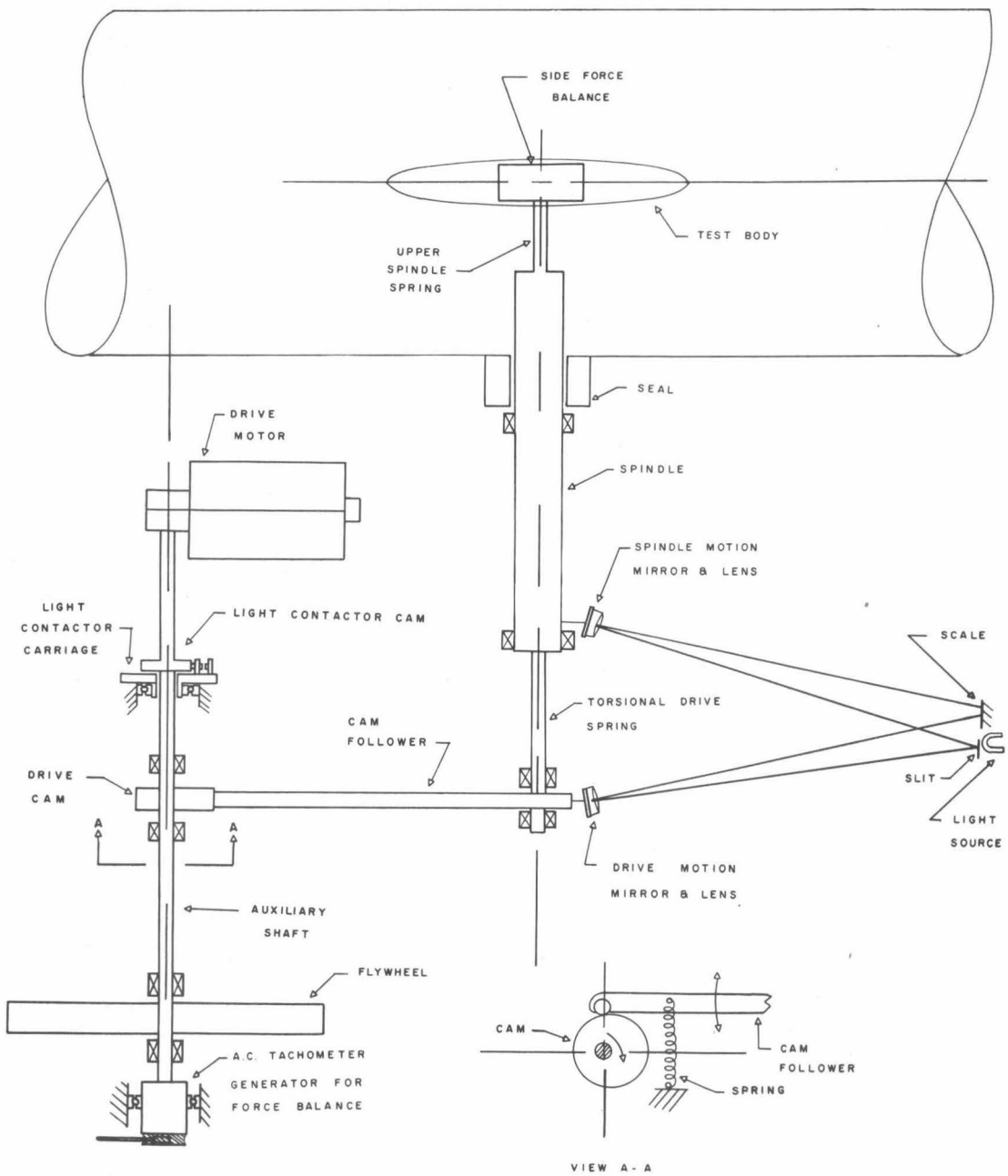

Fig. 3 - Schematic diagram of angular balance.

is not tightly sealed; the dimensions of the annular space are 0.001-inch radial clearance on a 0.875-inch diameter and one-inch length. At the typical tunnel static pressure of ten psig the water leakage is about ten gallons per hour. This water is collected by a vacuum system and is discarded before it can reach the spindle bearings.

Power is supplied by an a-c series motor which drives an auxiliary shaft. The speed of rotation determines the rate of forced angular oscillation of the test body and is held constant by the large moment of inertia of a flywheel and the action of a velocity feedback speed control system. The auxiliary shaft carries the main drive cam, the timing cam for controlling the flashing of a stroboscopic lamp, and an a-c tachometer generator. This last unit is used in the measurement of the lateral force. The main drive cam and its follower assembly convert the constant speed rotational motion of the auxiliary shaft into constant amplitude, constant frequency, sinusoidal oscillatory motion at a drive platform. The spindle carrying the test body is connected to this drive platform by a torsion spring. The diameter of a short section of the upper part of the spindle is small enough so that its torsional deflection must be considered.

The equations of motion of the forced angular motion are now formulated. An equivalent mechanical circuit of the angular motion is given in Fig. 4.

I, B, K — Moment of inertia, angular damping rate, angular spring rate of test body-fluid system

K_1 — Drive torsion spring rate

K_2 — Upper spindle torsion spring rate

I_s — Moment of inertia of spindle

B_s — Angular damping rate of spindle bearings, seal, etc.

$\beta = A_0 \sin(\omega t - \delta_0)$ Body motion

$\beta_1 = A_1 \sin(\omega t - \delta_1)$ Spindle motion

$\beta_2 = A_2 \sin(\omega t - \delta_2)$ Drive platform motion

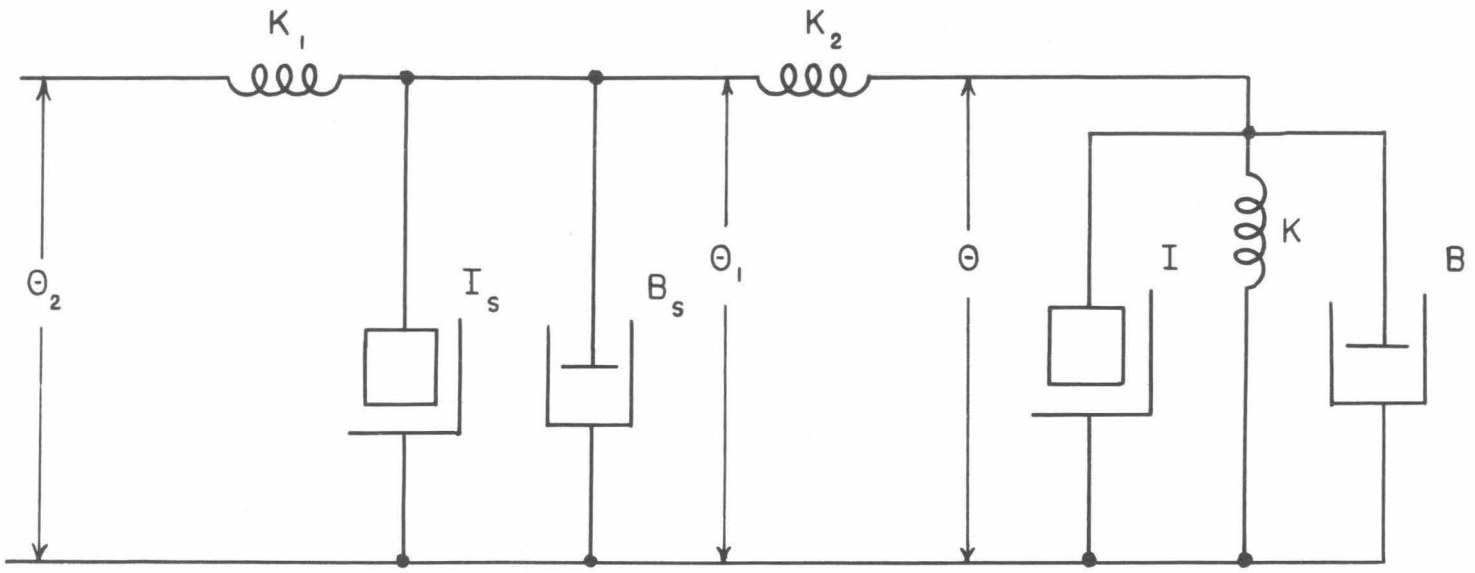

K_1	Drive spring rate	B_s	Damping rate of spindle seal
K_2	Spindle spring rate	I_s	Moment of inertia of spindle
K	Equivalent spring rate of fluid	θ	Motion of body
B	Equivalent damping rate of fluid	θ_1	Motion of spindle
I	Moment of inertia of body and fluid	θ_2	Motion of drive platform

Fig. 4 - Equivalent mechanical diagram of angular balance.

$$I_s \ddot{\beta}_1 + B_s \dot{\beta}_1 = K_1(\beta_2 - \beta_1) - K_2(\beta_1 - \beta) \tag{18}$$

$$I\ddot{\beta} + B\dot{\beta} + K\beta = K_2(\beta_1 - \beta). \tag{19}$$

Only the steady-state constant frequency solution is desired. The complex variable form of solution customary in steady-state alternating current problems is used.

$$\left\{ \frac{K_2 + K}{K_2} - \frac{I\omega^2}{K_2} + \frac{j\omega B}{K_2} \right\}^{-1} = \frac{K_1 + K_2}{K_2} - \frac{I_s\omega^2}{K_2} + \frac{j\omega B_s}{K_2} - \frac{K_1}{K_2}\frac{A_2}{A_1} \left\{ \cos(\delta_2 - \delta_1) - j \sin(\delta_2 - \delta_1) \right\} \tag{20}$$

Examination of this equation shows that the data necessary to compute the quantities I, B and K are the physical constants of the balance K_1, K_2, I_s, and B_s, and the frequency, amplitude ratio and relative phase angle of the drive platform and spindle motions. Measurements at two frequencies are necessary to separate the $(K - I\omega^2)$ term.

The amplitude and phase-angle of the test body motion are also desired. They are used in the lateral force measurement.

$$\frac{A_o}{A_2} \left\{ \cos(\delta_o - \delta_2) - j \sin(\delta_o - \delta_2) \right\} = -\frac{K_1}{K_2} + \left\{ \frac{K_1 + K_2}{K_2} - \frac{I_s\omega^2}{K_2} + \frac{j\omega B_s}{K_2} \right\} \left\{ \cos(\delta_1 - \delta_2) - j \sin(\delta_1 - \delta_2) \right\} \tag{21}$$

The measurement of K_1 and K_2 is made by static dead weight test. For design purposes the portion of B_s due to the fluid seal at the tunnel wall was computed assuming laminar flow in the annular space. The computed value of 6×10^{-6} lb ft sec is negligibly small in the equation. It was confirmed that the entire spindle damping term is negligible by a calibration run in still water in the tunnel. An umbrella-type shield was used so that the body moved in a pocket of air, and hydrodynamic damping was not present. Under these conditions the phase shift between the spindle and drive platform motions was less than 0.1 degree. The term B_s is now dropped

from the equations. The value of I_s is computed to be 5.9×10^{-5} lb ft sec^2. For all but the highest frequency runs of ten cps its contribution is also negligible.

The frequency of oscillation is determined by an electronic counter that measures the period of the output of the a-c tachometer generator. An extremely stable and accurately known rate of oscillation was desired to facilitate the measurement of the side force. Stability of 0.1 to 0.05 per cent at any set speed from 2 to 10 cps is achieved with the speed control system.

The amplitude ratio and phase angle are measured stroboscopically. Electrical contacts actuated by the timing cam on the auxiliary shaft are mounted on a carriage that can be rotated concentrically with this shaft. The angular position of the contacts determines the time in the cycle of motion of the flashing of a General Electric type Ft-110 flash tube. The short duration flash of light is reflected and focused by lens and mirror combinations mounted on the drive platform and spindle, and the images are formed on a curved scale about six feet away. The timing cam has two actuating surfaces spaced 180 degrees apart. One of two contact assemblies, spaced 90 degrees apart on the contact carriage, is selected by a switch, and two flashes of light occur for each cycle of motion at, for example, the zero and 180-degree points.

Two methods of taking data are available. In the shorter method, the contact carriage is rotated until the two flashes of light occurring 180 degrees apart are observed to coincide. The angular position of the carriage is a measure of the phase of the motion. The peak amplitude is then measured by switching to the other contacts. In the second method the actual wave form of the motion is taken and the amplitude and phase of the fundamental frequency motion are then determined by Fourier analysis. This latter method is used for all measurements of the spindle motion since this motion contains a greater or lesser amount of transient disturbances due to real fluid effects.

The inherent accuracy of measurement is estimated to be equal to or better than 0.5 percent for the amplitude ratio and 0.5 degree for the phase angle. The 180-degree spacing of the actuating surfaces on the timing cam, the 90-degree spacing of the two contact assemblies, and the rotation of the

contact carriage are checked by stroboscopic techniques against a primary set of marks on the perimeter of the flywheel. These quantities are all accurate to better than 0.1 degree. The width of the light image and the smallest division on the scale are equivalent to about 0.01 degree of angular rotation. Peak to peak amplitude of the drive platform motion is four degrees. The maximum amplitude ratio encountered under test conditions was about 1.6, corresponding to model and spindle total amplitudes of 6.5 degrees.

(b) Measurement of Lateral Force

The lateral force on the test body is measured by a spring balance structure located inside the center portion of the body. The essential features are shown in Fig. 5.

The outer shell of the balance proper is fastened to the spindle by means of a parallelogram flexure linkage which transmits only side force to the open-coil weighing spring, the moment reaction being taken out as tension and compression in the flexure links. For a maximum force of 3 lb and a spring constant of 3000 lb per in., the maximum lateral motion is about 0.001 in.; the fluid reaction of this motion is considered negligible compared to that of the angular motion. The natural frequency of this lateral degree of freedom based on one-pound weight of the body and assessed fluid is greater than 160 cps. For oscillation frequencies of less than 10 cps, the lateral motion is spring-controlled, and the instantaneous lateral deflection is proportional to the instantaneous lateral force.

The steady-state solution to equation (16) is used to separate the total lateral force into the components proportional to angular position, velocity and acceleration. This solution in complex variable form is given below:

F peak magnitude of lateral force

δ_f phase of lateral force relative to motion of body.

$$F(\cos \delta_f + j \sin \delta_f) = - \left[(k + m\omega^2) + j\omega b \right] A_o . \tag{22}$$

$$k + m\omega^2 = - \frac{F}{A_o} \cos \delta_f . \tag{23}$$

$$\omega b = - \frac{F}{A_o} \sin \delta_f . \tag{24}$$

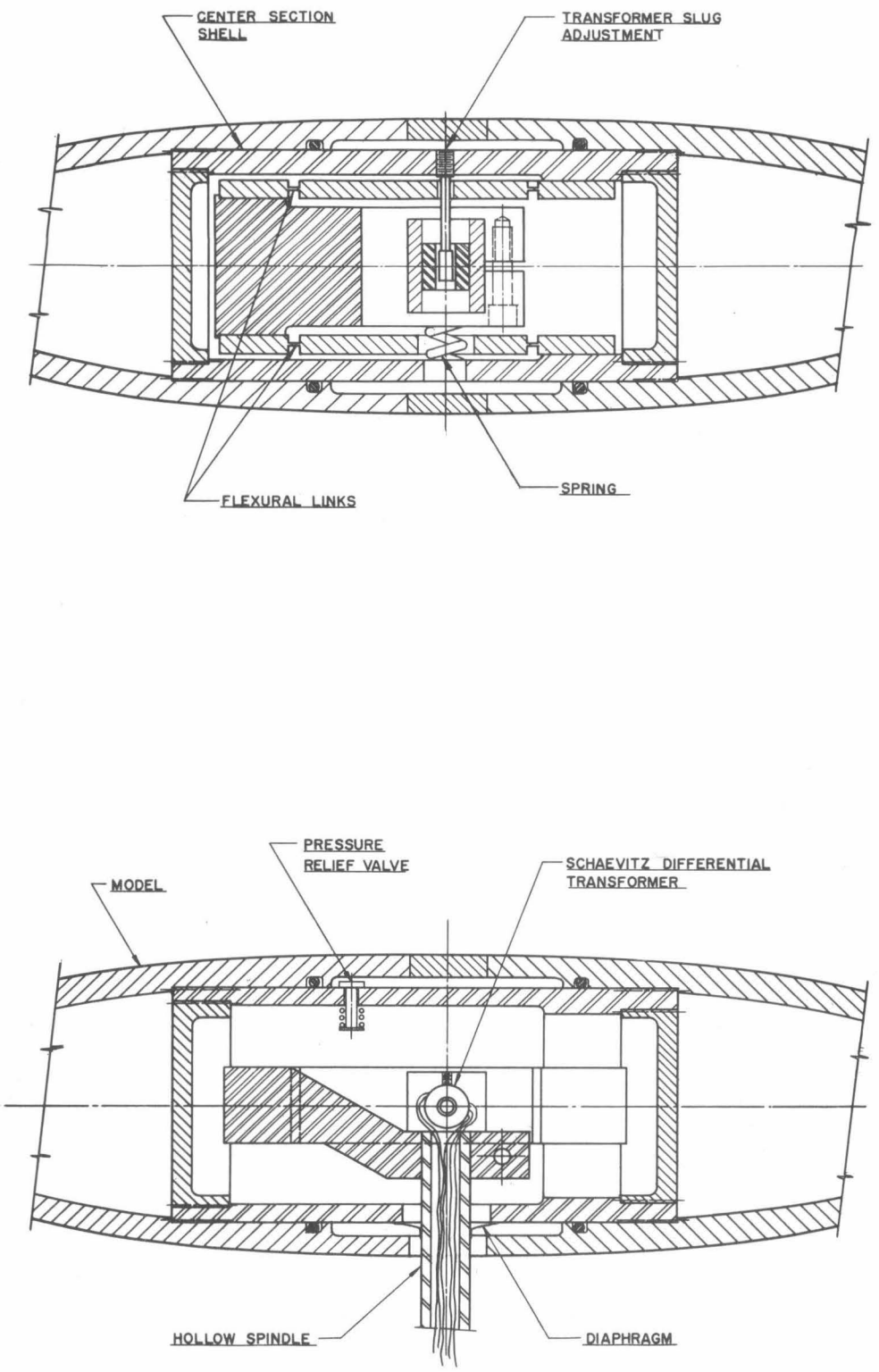

Fig. 5 - Schematic diagram of side force balance.

The electrical connections to the inside of the body are made through a hollow spindle to which the lateral balance section is fastened in a semi-permanent fashion. To insure against leakage of water into the balance section a rubber diaphragm is located between the spindle and the balance shell, also, dry air is supplied to the interior of the balance (via the hollow spindle) at a pressure several psi above the static pressure of the tunnel. The thin aluminum shells that formed the actual exterior surface of the ellipsoidal bodies were fitted over the lateral balance section.

The transducer element is a linear differential transformer which exhibits an output voltage proportional to the relative linear position of the center iron slug and its concentric winding. A carrier system with a center frequency of 1000 cps is used and the output voltage of the pickup is an amplitude modulated wave. The center position of the slug is set far enough from the electrical null so that the degree of modulation is less than 100 per cent for the maximum force to be measured. Figure 6 is a block diagram of the electronic equipment. The peak output of the pickup unit is on the order of millivolts. After suitable amplification, band-pass filtering, demodulation, and low-pass filtering, this voltage appears across a load resistor. It is a sinusoidal voltage whose magnitude is proportional to the magnitude of the side force and whose phase is the phase of the side force plus the frequency dependent phase shift of the filters and other circuits.

A null method is used to make the actual measurement. The output voltage of the a-c tachometer generator is added to the unknown voltage. The amplitude of the tachometer voltage is adjusted by attenuators and its phase by rotation of the generator frame until the sum of the two voltages is zero. The null condition is detected by passing the sum voltage through a twin-T feedback, narrow pass band, amplifier set to reject all frequencies except the frequency of oscillation. The output is displayed on an oscilloscope with the tachometer voltage used for the horizontal sweep. Errors in amplitude balance appear as a tilting of the pattern and errors in phase as an opening of the pattern into an ellipse. The extreme speed or frequency stability is required because of the rapid rate of phase shift of the twin-T amplifier if this method of indication of the type of voltage unbalance is to be usable.

Amplitude calibration of the side force balance is done by static test.

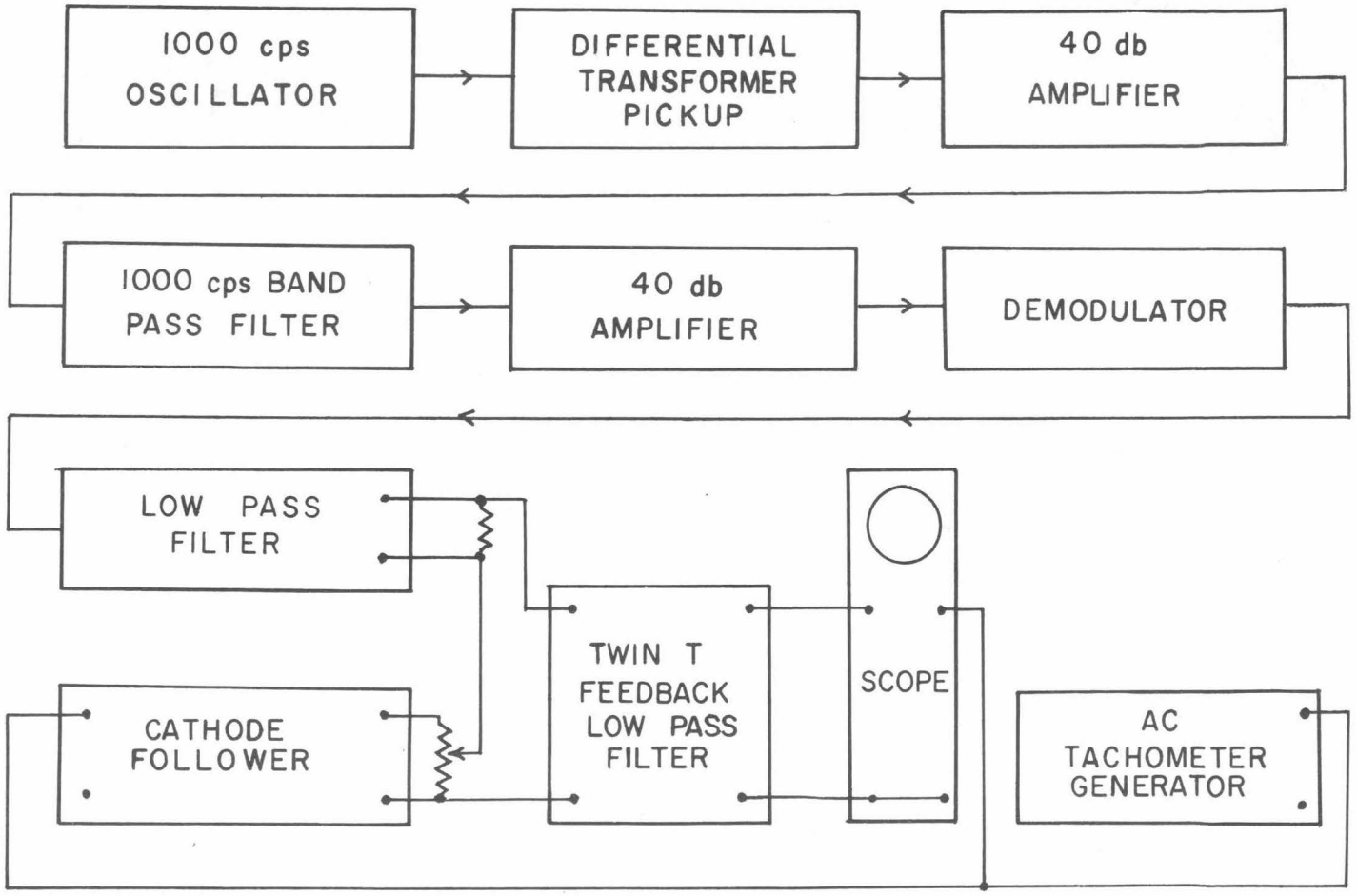

Fig. 6 - Block diagram of electronic equipment for side force balance.

Since all of the associated electronic equipment is operated on a relative basis no absolute measures of voltage are necessary; simple bridge type rectifiers and precision d-c meters are used to monitor the small changes in carrier voltage and amplifier gain. An oscilloscope is used to determine the connection between the phase of the a-c generator and the angular position of the flash lamp contacts in terms of which the motion of the test body is calculable. The phase shift of the electronic equipment is calculable and is verified by stroboscopic calibration. The over-all accuracies of the equipment and operational method is judged to be one per cent for amplitude and one degree for phase measurements.

(c) Discussion of the Experimental Method

A few remarks regarding several aspects of the steady-state forced oscillating motion experimental method have been deferred until now since they apply to both the linear cross-force and angular yawing moment measurements. The motivation for the use of the method, the several assumptions required to adapt it to the experimental program, and the limitations to be placed on the results will be discussed first. Then some of the quantitative aspects of the method will be given; particular emphasis will be placed on the factors that determine the degree of accuracy that may be attained.

In the making of many hydrodynamic measurements it is necessary to cope with the transient fluctuations, disturbances, and turbulence of the flow of real fluids. Some method of averaging is used to arrive at a mean or average value of the desired hydrodynamic quantities. For the static reactions of lift, moment, and drag on a body in a fluid, the situation is straightforward. The fluid flow is steady when viewed over an interval of time. The several reactions are precisely defined in terms of this time average description of the flow. The reactions possess true time averages which may be measured with static or very low frequency response gauges. When the magnitude of the fluctuating or transient effects are greater than the average values, these averages still exist and are even measurable, although they may no longer be meaningful or useful.

Fluid motions that give rise to damping and inertial type reactions are usually not steady in the sense that the simple time averaging process can

no longer be applied. As used here, the terms damping and inertial refer to those reactions caused by linear and angular acceleration and angular velocity. There are motions of the body and fluid in which reactions other than the static reactions do occur and that are steady in the sense that the reactions are independent of time. An example is steady forward linear velocity with constant rate of turning. In the general case, and in the particular case of motion of a body in the cylindrical working section of a constant velocity water tunnel, motions that give rise to damping and inertial reactions require some form of instantaneous, or at least time-dependent, measurement method.

In the present experimental program the coefficients of the fluid reactions due to yawing motion are desired. Only small amplitudes of yaw are to be permitted, and it is assumed that the fluid reactions are representable as linear functions with constant coefficients of the angle of yaw and its first and second time derivatives. This experimental situation is admirably suited to a steady-state periodic motion experimental method. The relative velocity and acceleration of the body and fluid necessary to produce the desired hydrodynamic reactions are available. The steady-state or repetitive nature of the motion permits the use of frequency selective instrumentation which can be made relatively insensitive to transient disturbances. Single frequency sinusoidal motion is a natural choice for the periodic motion. Its more important features are that position, velocity, and acceleration are smooth, continuous functions of time and are so related to each other that their separation into these components is easily accomplished. Rejection of the transient disturbances is done by Fourier analysis for the angular motion and conventional electric filter circuits for the lateral force. At the higher tunnel velocities and higher oscillation frequencies used, instantaneous deviations of about 15 per cent of the amplitude of the fundamental frequency of motion were encountered in the angular motion of the body. Yet measured values of the amplitude and phase of the fundamental motion from independently taken data differed by only two to three per cent at most. Of course, as the magnitudes of the transient disturbances increase it becomes more difficult to separate the desired information from the background noise. Finally, just as in the case of static reactions, the point is reached where the reaction proportional to the sinusoidal motion is so small compared with the other reactions that its

coefficient is of doubtful utility.

The harmonic content of the angular motion of the body and of the electrical signal proportional to the cross-force is also a measure of the correctness of the linearity assumption. A linear system excited or driven by a periodic motion can only amplify harmonics present in the driving motion. It cannot generate new ones. From the known harmonic content of the driving motion, the approximate content of the response motion may be estimated. The appearance of harmonics in considerable excess of this is indicative that the basic assumption of linearity does not hold and the experimental method cannot be used in its simple form.

The second topic to be discussed that is applicable to both the moment and force measurement is the accuracy of the determinations of the several hydrodynamic coefficients. In preceding sections of this report estimated accuracies for various measured quantities are given. These quantities are either primary data or simple arithmetic combinations of primary data. Their respective accuracies are determined from the scatter of individual data from the average of the data.

The reduction of these primary and intermediate data to hydrodynamic coefficients follows essentially the same pattern for both the force and moment measurement. For example, to obtain the force coefficients, equations (23) and (24) are used. The quantities k, b, and m have already been identified with the hydrodynamic coefficients. At least two runs are necessary to evaluate all three quantities. In actual practice, four or five runs at different frequencies of oscillation and at the same tunnel velocity are used. For each run a value of b is obtained. The quantity $(k + m\omega^2)$ obtained from each run is plotted versus the square of frequency and values of k and m determined from the intercept and slope of the line. The data reduction procedure is discussed in detail later.

It is in these separation steps that considerable accuracy may be lost. Actually, it is more correct to say that the potentiality for high accuracy was never present. When a particular component or part of a total reaction is not large enough compared with the other components to affect the total reaction significantly, a measurement of the total reaction cannot give so accurate a measure of it as it can of the other larger components. In a

spring-damping-inertia system, for example, for this type of steady-state measurement of amplitude and phase angle, the significant parameters are the natural frequency and critical damping. For highly damped systems, the motion is damping controlled over a large range of frequencies, centered at the natural frequency. Good measure of the damping component can be realized. On the other hand, it may be necessary to go to very low frequencies for a spring rate measurement or to very high frequencies for an inertial measurement of comparable accuracy. At the other extreme of lightly damped systems, it would not be necessary to go as low below the natural frequency for a good spring measurement, or, conversely, as high above for the inertial component, but now the damping component may be difficult to get because of the higher amplitude of motion near resonance.

Although neither the moment nor cross-force system of this experiment matches the sample system just described, the situations with regard to accuracy of separation into components are very similar. A total reaction is measured; the separation accuracy is determined to a large degree by the relative magnitude of the components. Since linearity with amplitude is assumed, the only variable parameter is the frequency of oscillation, and since the relative magnitudes do depend on frequency, this procedure may be used to permit better determination of one of the smaller components.

It may be pointed out here that if k, b or m are functions of reduced frequency, the experimental method may still be used. The primary requirement of the method is linearity and superposition of the three components of the reaction; it is equation (7) that must be valid. The data reduction is somewhat different when there is dependence on reduced frequency, Reynolds number, or other dimensionless quantities. A value of b is still determined for each run in the way previously described. It is then the reduction of this value to a dimensionless coefficient that may involve the dimensionless parameters. When the $(k + m\omega^2)$ term is plotted versus the square of frequency its slope may no longer be constant,and values of k and m may have to be determined for each point. Then, after this separation step, the reduction of k and m to dimensionless coefficients may involve several dimensionless parameters.

The preceding paragraphs were intended to be a brief, yet sufficiently complete, exposition of the data reduction procedures to enable the reader to appreciate both the possibilities and limitations of the experimental method. In order for it to be used to determine a specified hydrodynamic

coefficient, it is first necessary that a steady-state motion be devised in which the desired reaction appears in a linear form. Nonlinear terms must be sufficiently small so that the linear terms are not affected. Then the balance must be operated over a sufficiently wide range of fluid velocities and oscillation frequencies to separate the reaction to a desired degree of accuracy from other reactions. Finally this reaction must be reduced to the desired dimensionless coefficient, including the discovery of any appropriate dimensionless parameters. The reader will recognize that the ease or difficulty of the task may vary considerably from one body shape to another or from one coefficient to another for the same body.

EXPERIMENTAL RESULTS

Test Conditions

Experimental tests were made with three prolate ellipsoidal shapes. The three test bodies were each two inches in diameter and six, ten, or fourteen inches long. They are referred to as the 3:1, 5:1, and 7:1 bodies, respectively. The outer shells were made of aluminum and the wall sections were made as thin as possible to minimize their moments of inertia, over-all dimensional tolerances having been held to approximately ± 0.001 inch. The external surface was polished to about a five micro-inch finish.

The velocity of the water in the tunnel was varied in increments of 5 fps in the range from 0 to 25 fps, while the tunnel pressure was held between 5 and 10 psi gauge.

These pressures were high enough to prevent cavitation at all tunnel velocities, and the accidental pressure variations within the observed range of fluctuations did not produce any measurable changes in the fluid reactions on the body.

Frequencies of angular oscillation of two, four, six, eight, and nine or ten cycles per sec were used. The half amplitude of the drive motion was two degrees, and the amplitudes of the motion of the test bodies varied with frequency and tunnel velocity. The maximum half amplitudes were about 3.2 degrees.

The spindle supporting the test bodies was surrounded by a smooth symmetrical airfoil shield. The effect of this shield can be roughly

estimated by placing a second image shield on the opposite side and assuming that the effects of two shields are twice the effects of the single shield. This was done for several runs. The effects were on the order of several percent. They were not applied to the data but reference is made to the direction of the changes in the discussion of the results.

Data Reduction

The several items of primary data are reduced to intermediate curves and data by equation (20) for the angular reaction, and equation (22) or equations (23) and (24) for the lateral reaction. It is seen that the procedures for the separation of the total reaction into its several components is essentially the same for both the moment and force measurements. The data is first separated into a damping or velocity component and position-acceleration component. Mathematically this is accomplished by the separation of the complex equations (20) and (22) into their real and imaginary parts.

The hydrodynamic coefficients are computed from the slopes and intercepts of the data reduction curves. When these curves are straight lines, one numerical value independent of frequency of oscillation is obtained for each coefficient for each tunnel velocity. When the curves are not straight lines, the same general form of data reduction is used, but now the values obtained for the coefficients apply only to specific values or ranges of values of tunnel velocity and oscillation frequency.

The coefficients obtained in both of the above cases are reduced to dimensionless form according to the standard nomenclature and presented in figures plotted versus tunnel velocity or Reynolds number based on the product of velocity and length. When the coefficients in these final plots are constant independent of tunnel velocity, and when they have come from straight line data reduction curves, it may be concluded that the coefficients are independent of both Reynolds number and reduced frequency.

Experimental Results

The static moment coefficients, N_v', and the virtual moment of inertia coefficients, $N_{\dot{r}}'$, are computed from the data reduction curves of Fig. 7. Their values are given in Figs. 10 and 11. These reactions exist in a perfect fluid and the perfect fluid values are given in the figures.

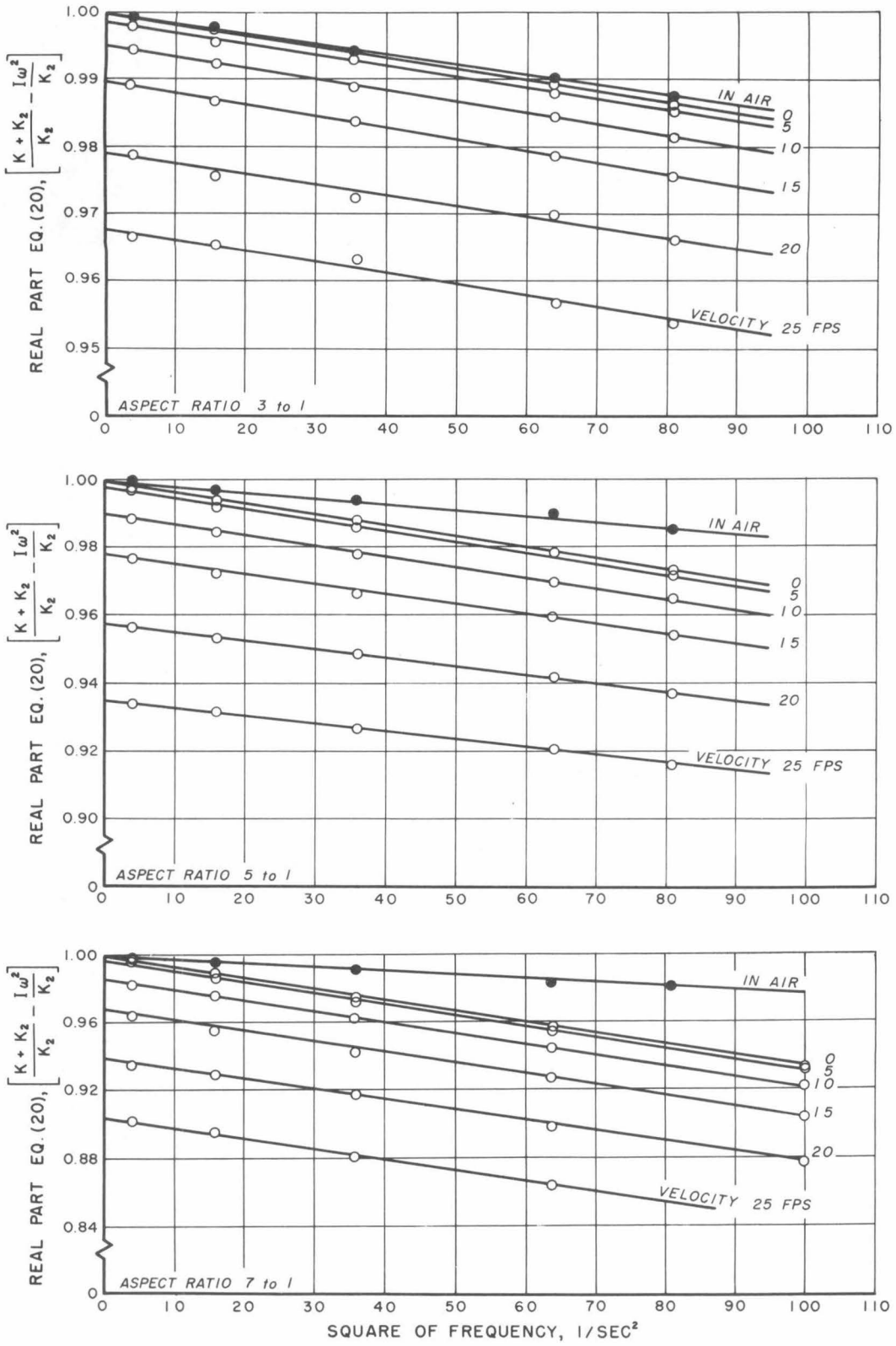

Fig. 7 - Data reduction curves used to obtain static moment coefficients and virtual moment of inertia coefficients.

The magnitude of the moment due to angular velocity was small compared with the magnitudes of the static and acceleration reactions. The phase angles were usually less than one degree and could not be determined with any accuracy. The usual data reduction curve was not made. The magnitude of its coefficient ($N_r' - N_{\dot{v}}'$) was estimated and is given in Fig.13. These values must be considered as order of magnitude only. This reaction is zero in a perfect fluid.

The coefficients of static lift, Y_v', and of lift due to angular acceleration, $Y_{\dot{r}}'$, are given in Figs. 14 and 15. They are calculated from Fig. 8. The lines in these data reduction curves are not straight. The lift coefficients of Fig. 14 are based on the intercepts at zero frequency of the faired curves. The acceleration coefficients of Fig. 15 are based on the slopes of the straight lines at the higher frequencies of oscillation. Both of these reactions are zero in a perfect fluid.

The damping lift coefficients, $Y_r' - Y_{\dot{v}}'$, are computed from the data curves of Fig. 9. They are given in Fig. 12 along with the perfect fluid values.

Conclusions

The relative magnitudes of the three components of the lateral force were such that good separation of it into these individual reactions was possible over almost the entire frequency and tunnel velocity ranges.

The data reduction curves of Fig. 8, from which the coefficients of static lateral force or lift and of lateral force due to angular acceleration were taken, have pronounced curvature at the low frequencies of oscillation. They do become straight lines at the higher frequencies. The lift coefficients of Fig. 14 were taken from the intercepts of the curves as extrapolated to zero frequency. These values should be directly comparable to true static coefficients taken at constant angle of attack. They are presented versus a Reynolds number. Their type and degree of dependence on Reynolds number is not unexpected.

The coefficients of lift due to angular acceleration are taken from the higher frequency runs where it appears that they are independent of frequency over a considerable range. These are plotted versus Reynolds number in Fig. 15. Again, since this reaction is zero for perfect fluids, a dependence

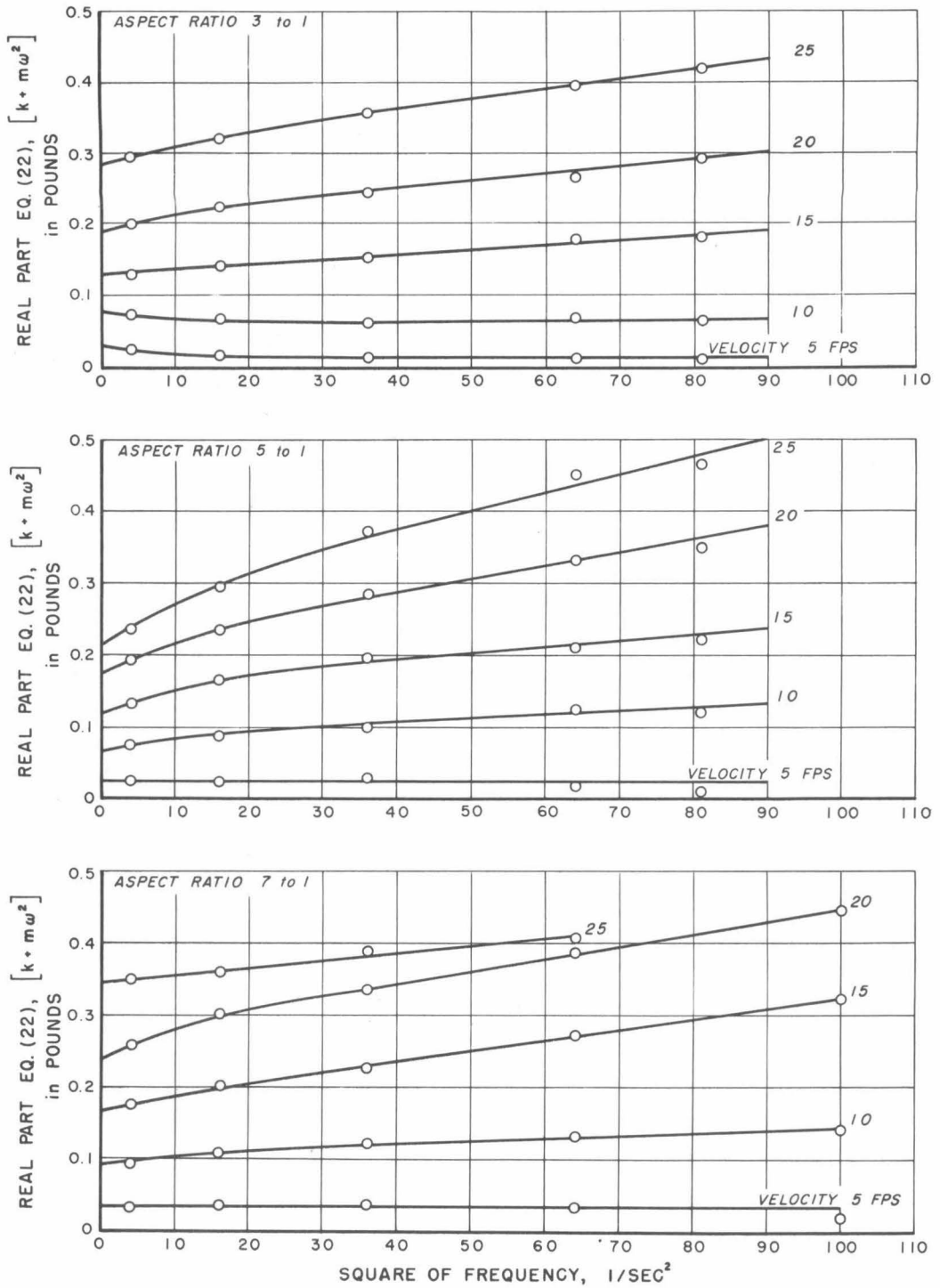

Fig. 8 - Data reduction curves used to obtain static lift coefficients and coefficient of lift due to angular acceleration.

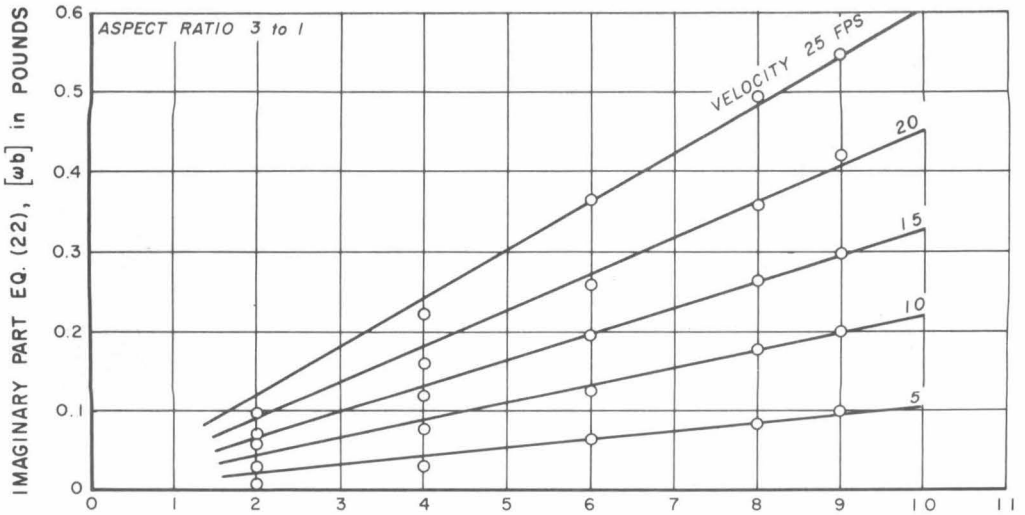

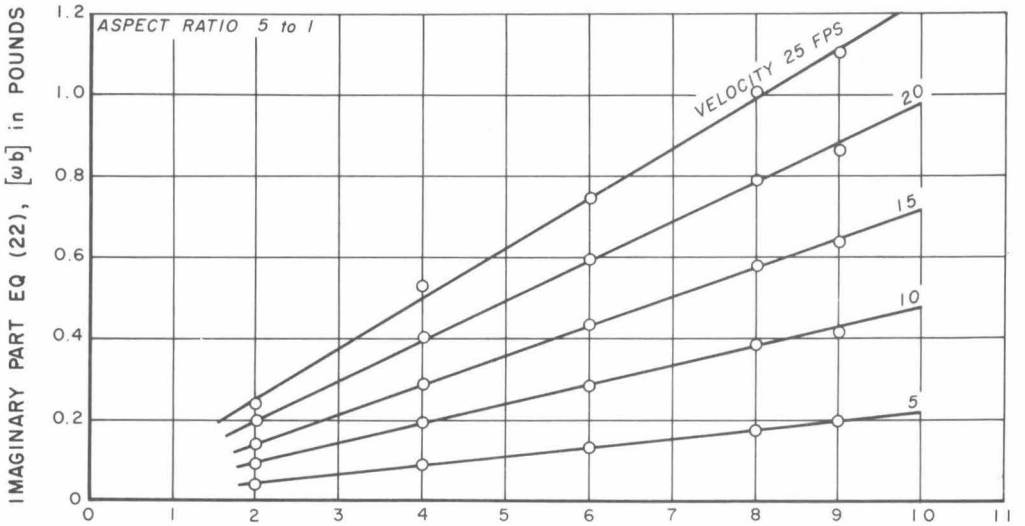

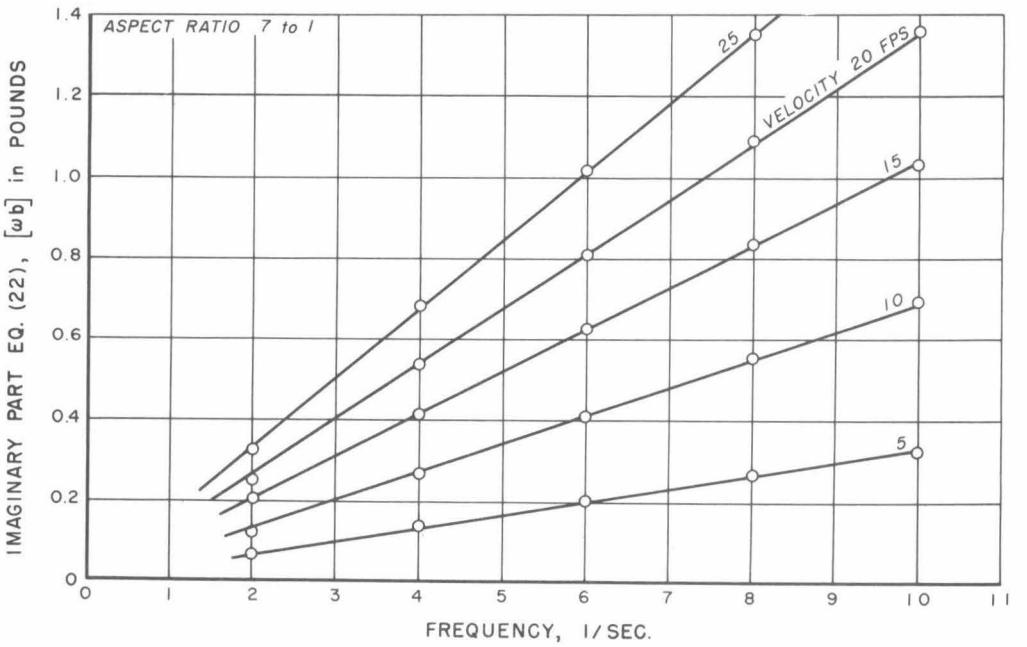

Fig. 9 - Data reduction curves used to obtain damping lift coefficient

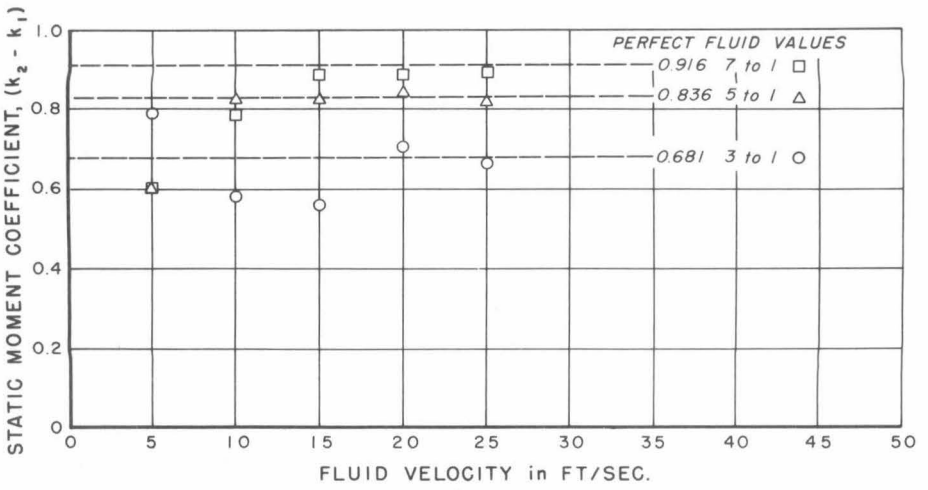

Fig. 10 - Static moment coefficient as a function of fluid velocity.

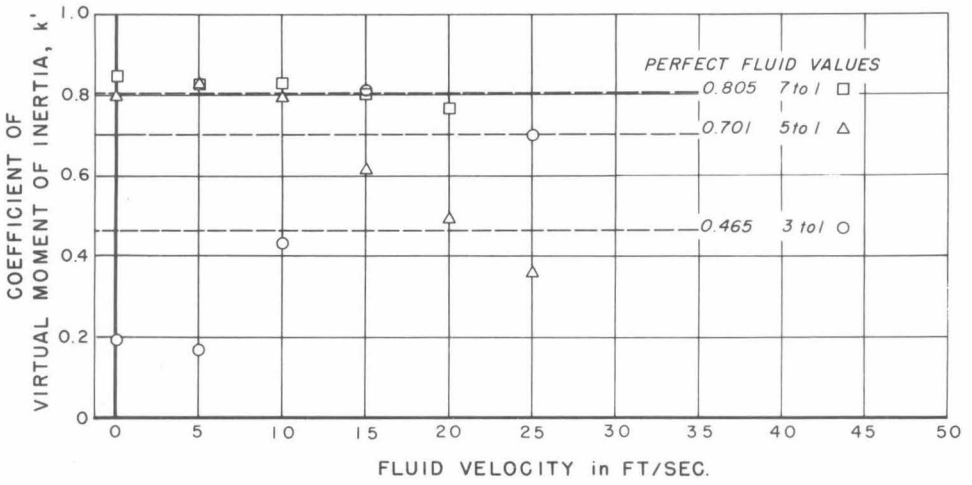

Fig. 11 - Coefficient of virtual moment of inertia as a function of fluid velocity.

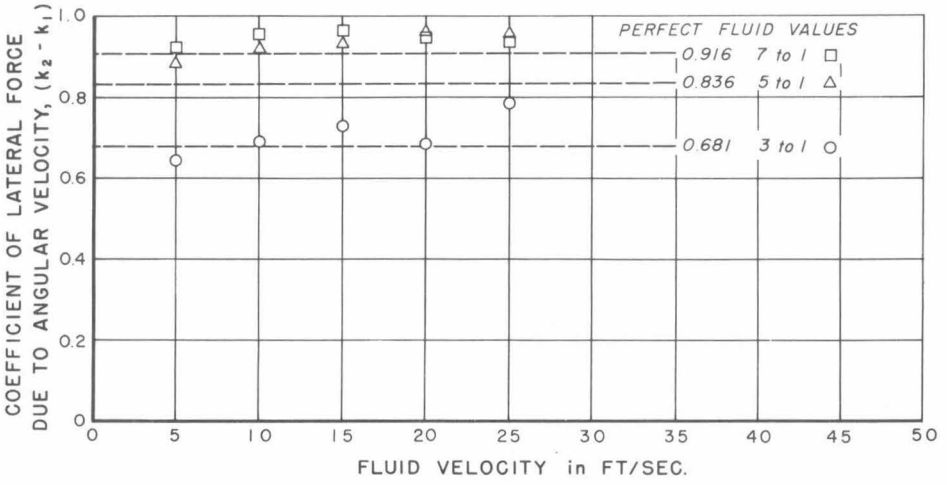

Fig. 12 - Coefficient of lateral force due to angular velocity as a function of fluid velocity.

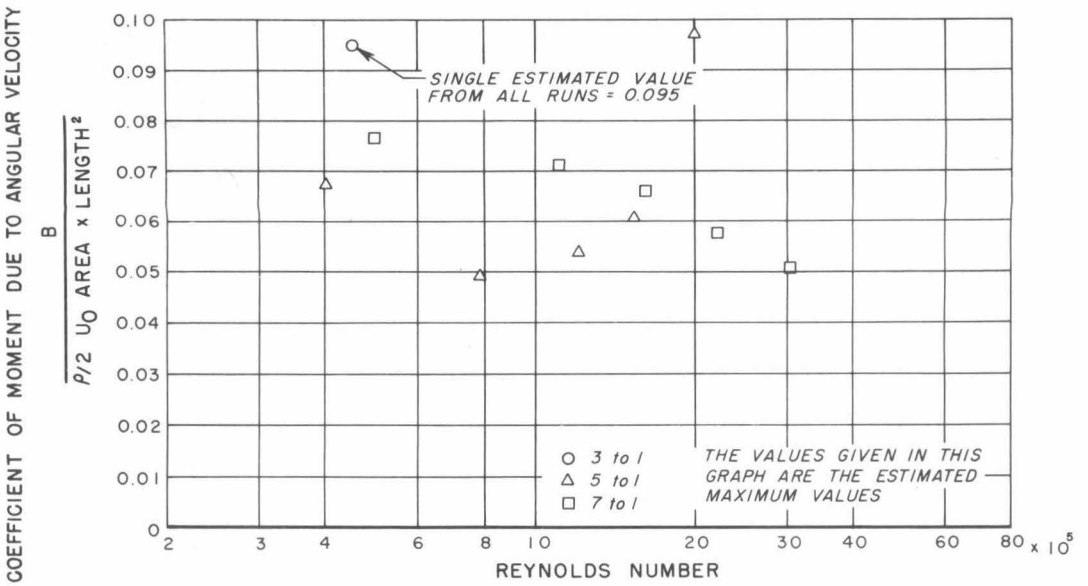

Fig. 13 - Estimated values of coefficient of moment due to angular velocity as a function of Reynolds number.

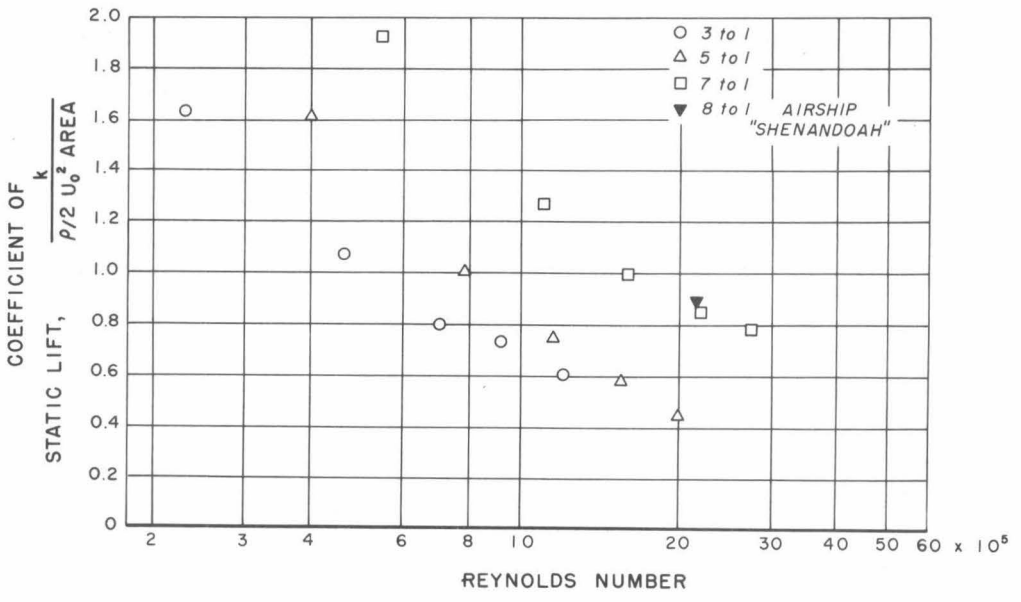

Fig. 14 - Coefficient of static lift as a function of Reynolds number.

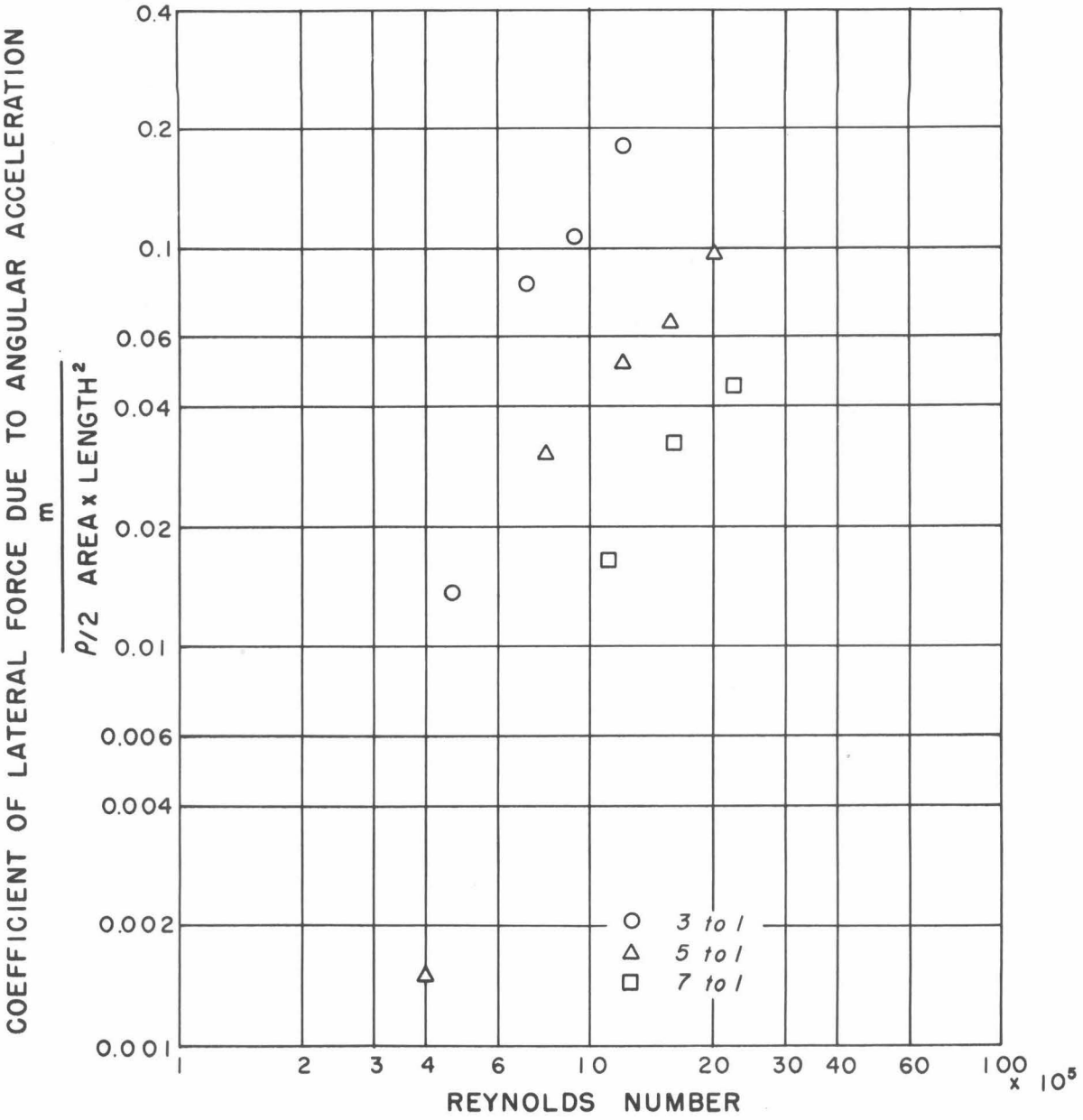

Fig. 15 - Coefficient of lateral (lift) force due to angular acceleration as a function of Reynolds number.

on Reynolds number is not unexpected. Except for the points at the lowest tunnel velocity of five feet per second, this coefficient seems to be linearly proportional to Reynolds number over the range of tunnel velocities.

No further interpretation of these data reduction curves is attempted. It is felt that additional data are necessary. Particularly needed are data in which the Reynolds number variation is caused by changes in viscosity. The curvature at the low frequencies should then be examined for a dependence on reduced frequency as well.

The coefficient of lateral force due to angular velocity is given in Fig. 12. The data reduction curves are straight lines and the dimensionless coefficients in the figure show no significant dependence on tunnel velocity. It is concluded that this coefficient is independent of reduced frequency and Reynolds number over the experimental range. This reaction exists in a perfect fluid and the values of the perfect fluid coefficients are given in the figure. The experimental values are all higher than these except for the single run at 5 cps for the 3:1 body. The shield connection, which has not been applied, would lower the experimental values a few per cent but still would leave most of them about three to five per cent above the perfect fluid values. It is concluded that this reaction is primarily a perfect fluid reaction and is not significantly modified by viscosity for motion in water over the range of the experiment.

The measurement of the angular quantities was made difficult by the large negative or destabilizing static moment rate and low damping rate of the prolate ellipsoidal shape. The balance had to be operated at frequencies well below the natural frequency of the system, and the resulting amplitude ratios of the drive and model motion changed from unity to only 1.4 over the entire frequency range. The phase angles were always small and not accurately measurable. The separation of the components of moment required the subtraction of nearly equal quantities with a resulting loss in accuracy.

The static moment coefficients of Fig. 10 become relatively less accurate in their determination, the smaller the tunnel velocities and the smaller the diameter-to-length ratio of the body, for reasons outlined in the previous paragraph. At the higher tunnel velocities the values for the 7:1 and 5:1 bodies are in good agreement with the perfect fluid values. The data reduction curves were straight lines and at the higher tunnel velocities

the coefficients are independent of velocity. No dependence on Reynolds number or reduced frequency is indicated.

The coefficients of virtual moment of inertia in Fig. 11 show a large dependence on tunnel velocity. The values for the 3:1 body must be completely disregarded. It can be seen from the data reduction curve of Fig. 7 that its virtual moment of inertia is so small compared with the moment of inertia of the body that accuracy of determination of the former is nil. For the 7:1 and 5:1 bodies the virtual inertia is at least of the same order of magnitude as that of the test bodies themselves. Sufficient accuracy remains so that the indicated decrease in the value of the coefficient with increasing velocity appears to be genuine. This inertial reaction is present in a perfect fluid and its coefficient is independent of tunnel velocity. This value is given in the figure. For the experimental work in the real fluid, the data reduction curves were reasonably straight lines indicating no major dependence on reduced frequency. The curvature in the figure indicates a strong dependence on Reynolds number. Again more data, especially at different viscosities of the fluid, are necessary to evaluate the effect.

The values of the coefficient of moment due to angular velocity in Fig. 13 are estimated values only. For the 3:1 body only one estimate covering the entire velocity range was made. Individual estimates were made for each tunnel velocity for the 5:1 and 7:1 bodies. Although these form somewhat smooth curves versus Reynolds number, no attempt at correlation should be made. These values are to be considered as order of magnitude estimates only.

REFERENCES

1. Milne-Thomson, L. M., Theoretical Hydrodynamics, Macmillan and Company, 1949, pp. 477 - 481.

2. Lamb, Sir Horace, Hydrodynamics, Dover Publications, New York, 1945 (Sixth Edition).

3. Zahm, A. F., Smith, R. H., and Louden, F. A., "Air Forces, Moments, and Damping on Model of Fleet Airship Shenandoah," NACA Report No. 215, Sept. 1925. Data from Table XX, p. 23.

APPENDIX I

NOMENCLATURE

The motion of the test body is restricted to the plane of yaw.

The symbols used to describe this motion and the associated hydrodynamic reactions on the body are in the greater part identical to those recommended in the Technical and Research Bulletin N. 1-5 of the Society of Naval Architects and Marine Engineers titled "Nomenclature for Treating the Motion of a Submerged Body through a Fluid". These symbols are marked with an asterisk (*) in the following list.

All units are in the pound-foot-second system.

	A_o, A_1, A_2	peak half amplitudes of motion of body spindle, and drive platform
	B_s	angular damping rate of spindle seal
	$B = -(N_r - N_{\dot{v}} U)$	damping coefficient in equation (8)
	F	peak magnitude of lateral force
	$I = I_b + I_f$	
	I_b	moment of inertia of body
	$I_f = -N_{\dot{r}}$	acceleration coefficient in equation (8)
	I_o	moment of inertia of displaced fluid
	I_s	moment of inertia of spindle
	$K = N_v U$	position coefficient in equation (8)
	K_1	spring rate of angular drive spring
	K_2	spring rate of upper portion of spindle
	M_o	mass of displaced fluid
*	N	hydrodynamic moment on body
*	$N_r = \frac{1}{2}\rho \ell^4 U N_r'$	rotary moment derivative
*	$N_{\dot{r}} = \frac{1}{2}\rho \ell^5 N_{\dot{r}}'$	virtual moment of inertia coefficient
*	$N_v = \frac{1}{2}\rho \ell^3 U N_v'$	static moment derivative

*	$N_{\dot{v}} = \frac{1}{2}\rho\ell^4 N_{\dot{v}}'$	virtual moment of inertia coefficient
	N_s	moment on body supplied by support
*	O	origin of body axes
*	U	linear velocity of body axes relative to fluid
	U, V, U_o, V_o	velocity of fluid at infinity in Appendix II
*	Y	hydrodynamic lateral force on body
*	$Y_r = \frac{1}{2}\rho\ell^3 U Y_r'$	rotary force derivative
*	$Y_{\dot{r}} = \frac{1}{2}\rho\ell^4 Y_{\dot{r}}'$	virtual inertia coefficient
*	$Y_v = \frac{1}{2}\rho\ell^2 U Y_v'$	static force derivative
*	$Y_{\dot{v}} = \frac{1}{2}\rho\ell^3 Y_{\dot{v}}'$	virtual inertia coefficient
	Y_s	lateral force on body supplied by support
	a	ellipsoid major semi-axis (in Appendix II only).
	$b = Y_r - Y_{\dot{v}} U$	damping coefficient in equation (7)
	b	ellipsoid minor semi-axis (in Appendix II only).
*	g	acceleration of gravity
	$\bar{i}, \bar{j}, \bar{k}$	unit vectors
	$j = \sqrt{-1}$	
	$k = - Y_v U$	position coefficient in equation (7)
	k'	perfect fluid virtual inertia coefficient moment of inertia
	k_1, k_2	perfect fluid virtual inertia coefficients x, y directions of motion
	$m = - Y_{\dot{r}}$	acceleration coefficient in equation (7)
*	r	angular velocity of body
*	t	time
*	u, v	linear velocity of body
*	x, y	body axes

*	x_o, y_o	fixed axes
*	β, β_1, β_2	angle of yaw of body, angle of spindle, angle of drive platform
	δ_o, δ_1, δ_2	phase of motion of body, spindle, drive platform
	δ_f	phase of lateral force
	$\omega = 2 \pi f$	angular frequency of angular motion; in Appendix II, only, angular velocity, r .
*	ℓ	length of body
*	ρ	density of fluid

APPENDIX II

Two-Dimensional Motion of a Prolate Ellipsoid in a Frictionless Fluid

Prolate Ellipsoidal Coordinates:

$$x = c\,\eta\,\xi\,, \quad y = r\cos\zeta\,, \quad z = r\sin\zeta\,,$$

$$r^2 = c^2\,(1 - \xi^2)\,(\eta^2 - 1)\,.$$

The boundary of the prolate ellipsoid represented by the equation

$$\frac{x^2}{a^2} + \frac{y^2}{b^2} + \frac{z^2}{b^2} = 1$$

is defined by the single ellipsoidal coordinate

$$\eta = \eta_o = \frac{a}{c}\,, \qquad c^2 = a^2 - b^2\,.$$

Let the geometric center, $x = y = z = 0$, be the origin of body axes. Motion takes place in the x_o, y_o coordinate system. The motion is described as follows:

u, v	components of body velocity resolved along body axes,
ω	angular velocity of body,
U, V	components of the velocity of the fluid at a large distance from the body resolved along body axes.

The velocity potential, ϕ, for this motion is

$$\phi = c\,u\,A_1\,P_1(\xi)\,Q_1(\eta) + c\,v\,A_2\,P_1^1(\xi)\,Q_1^1(\eta)\cos\zeta$$

$$+ c^2\,\omega\,A_3\,P_2^1(\xi)\,Q_2^1(\eta)\cos\zeta$$

$$- c\,U\left[A_1\,Q_1(\eta) + P_1(\eta)\right]P_1(\xi)$$

$$- c\,V\left[A_2\,Q_1^1(\eta) + P_1^1(\eta)\right]P_1^1(\xi)\cos\zeta\,.$$

$$A_1 = -\frac{1}{\dfrac{d\,Q_1(\eta_o)}{d\,\eta}}\,, \qquad A_2 = -\frac{\eta_o}{P_1^1(\eta_o)\dfrac{d\,Q_1^1(\eta_o)}{d\,\eta}}$$

$$A_3 = - \frac{P_1(\eta_o)}{P_2^1(\eta_o) \frac{d\, Q_2^1(\eta_o)}{d\, \eta}}$$

The P and Q functions are Legendre's polynomials.

Define:

$$k_1 = \frac{Q_1(\eta_o)}{P_1(\eta_o)} A_1 \quad , \quad k_2 = \frac{Q_1^1(\eta_o)}{P_1^1(\eta_o)} A_2 \quad ,$$

$$k' = \frac{9}{2\eta_o^2 - 1} \frac{Q_2^1(\eta_o)}{P_2^1(\eta_o)} A_3 \quad .$$

Choose $\eta = \eta_o$, $\xi = 1$ as a reference point on the surface of the body. The pressure equation derived for moving axes is

$$\frac{p}{\rho} + \frac{1}{2} q_r^2 - \frac{\partial \phi}{\partial t} - \frac{1}{2} q_b^2 = C(t) \, ,$$

where

$\overline{q}_b$ velocity of body,

$\overline{q} = - \overline{\nabla} \phi$ velocity of fluid,

$\overline{q}_r = \overline{q} - \overline{q}_b$ relative velocity.

The values of the quantities in the pressure equation are now given.

$$q_b^2 = u^2 + v^2 - 2 c u \omega (1 - \xi^2)^{1/2} (\eta_o^2 - 1)^{1/2} \cos \zeta$$

$$+ 2 c v \omega \eta_o \xi + c^2 \omega^2 \left\{ \eta_o^2 \xi^2 + (\eta_o^2 - 1)(1 - \xi^2) \right\} \cos^2 \zeta$$

$$q_b^2 \Big|_{\xi=1} = u^2 + (v + c \eta_o \omega)^2$$

$$q_r^2 = \frac{\eta_o^2 (1 - \xi^2)}{(\eta_o^2 - \xi^2)} (k_1 + 1)^2 (U - u)^2 \quad +$$

$$+ \left\{ \frac{\xi^2 (\eta_o^2 - 1) \cos^2 \zeta}{(\eta_o^2 - \xi^2)} + \sin^2 \zeta \right\} (k_2 + 1)^2 (v - V)^2$$

$$+ \frac{2 \eta_o \xi (1 - \xi^2)^{1/2} (\eta_o^2 - 1)^{1/2}}{(\eta_o^2 - \xi^2)} (k_1 + 1)(k_2 + 1).$$

$$(U - u)(v - V) \cos \zeta$$

$$+ \left\{ \frac{(\eta_o^2 - 1) \eta_o^2}{(\eta_o^2 - \xi^2)} \left[(2\eta_o^2 - 1)(1 - 2\xi^2) k' - 1 \right]^2 \cos^2 \zeta \right.$$

$$\left. + \eta_o^2 \xi^2 \left[(2\eta_o^2 - 1) k' + 1 \right]^2 \sin^2 \zeta \right\} c^2 \omega^2$$

$$- \frac{2\eta_o^2 (\eta_o^2 - 1)^{1/2} (1 - \xi^2)^{1/2}}{(\eta_o^2 - \xi^2)} \left[(2\eta_o^2 - 1)(1 - 2\xi^2) k' - 1 \right] .$$

$$(k_1 + 1)(U - u) c \omega \cos \zeta +$$

$$\left\{ \frac{-2 \eta_o \xi (\eta_o^2 - 1)}{(\eta_o^2 - \xi^2)} \left[(2\eta_o^2 - 1)(1 - 2\xi^2) k' - 1 \right] \cos^2 \zeta \right.$$

$$\left. + 2 \eta_o \xi \left[(2\eta_o^2 - 1) k' + 1 \right] \sin^2 \zeta \right\}$$

$$(k_2 + 1)(v - V) c \omega$$

$$q_r^2 \Big|_{\xi=1} = \left\{ (k_2 + 1)(v - V) + \eta_o \left[(2\eta_o^2 - 1) k' + 1 \right] c \omega \right\}^2$$

$$\frac{\partial \phi}{\partial t} = c \dot{u} k_1 \xi \eta_o + c \dot{v} k_2 (\eta_o^2 - 1)^{1/2} (1 - \xi^2)^{1/2} \cos \zeta$$

$$+ c \dot{\omega} k' (2\eta_o^2 - 1)(\eta_o^2 - 1)^{1/2} (1 - \xi^2)^{1/2} \eta_o \xi \cos \zeta$$

$$- c \dot{U} (k_1 + 1) \eta_o \xi$$

$$- c \dot{V} (k_2 + 1) (\eta_o^2 - 1)^{1/2} (1 - \xi^2)^{1/2} \cos \zeta$$

$$\left.\frac{\partial \phi}{\partial t}\right|_{\xi=1} = c \dot{u} k_1 \eta_o - c \dot{U} (k_1 + 1) \eta_o$$

The relationships between the directions and magnitudes of the unit vectors $\bar{i}$, $\bar{j}$, $\bar{k}$, $\bar{\xi}$, $\bar{\eta}$, and $\bar{\zeta}$ are now given.

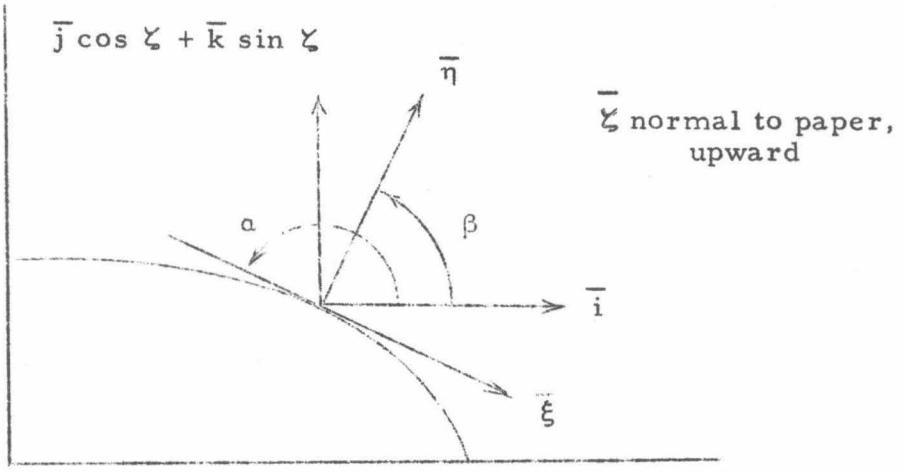

$$\tan \alpha = \frac{dr}{dx} = - \frac{b}{a} \frac{x}{(a^2 - x^2)^{1/2}} = - \frac{\xi (\eta_o^2 - 1)^{1/2}}{\eta_o (1 - \xi^2)^{1/2}}$$

$$\beta = \alpha - \frac{\pi}{2}$$

$$\cos \beta = \frac{\xi (\eta_o^2 - 1)^{1/2}}{(\eta_o^2 - \xi^2)^{1/2}} , \quad \sin \beta = \frac{\eta_o (1 - \xi^2)^{1/2}}{(\eta_o^2 - \xi^2)^{1/2}}$$

The element of surface area, dS, is given by

$$dS = c^2 (\eta_o^2 - \xi^2)^{1/2} (\eta_o^2 - 1)^{1/2} \, d\xi \, d\zeta \quad .$$

The force and moment exerted on the body by the fluid are now given.

$$X = f_x = \int_S - p \cos\beta \; dS = \int_{-1}^{+1} \int_0^{2\pi} - p\, c^2 (\eta_o^2 - 1)\, \xi \, d\xi \, d\zeta$$

$$= \frac{4}{3} \rho\, c^3\, \eta_o (\eta_o^2 - 1) \left\{ (\dot{U} - \dot{u})\, k_1 + \dot{U} + (v - V)\, k_2\, \omega - V\, \omega \right\}$$

$$Y = f_y = \frac{4}{3} \rho\, c^3\, \eta_o (\eta_o^2 - 1) \left\{ (\dot{V} - \dot{v})\, k_2 + \dot{V} - (u - U)\, k_1\, \omega + U\, \omega \right\}$$

$$Z = 0$$

$$N = \int_S (- y\, dX + x\, dY)$$

$$= - \frac{4}{15} \rho\, c^5\, \eta_o (\eta_o^2 - 1)(2\eta_o^2 - 1)\, k'\, \dot{\omega}$$

$$- \frac{4}{3} \rho\, c^3\, \eta_o (\eta_o^2 - 1)(k_2 - k_1)(u - U)(v - V) .$$

When the values of c and η_o are replaced by a and b and the mass, M_o, and moment of inertia, I_o, of the displaced fluid are calculated, these equations become

$$X = M_o \left\{ (\dot{U} - \dot{u})\, k_1 + \dot{U} + (v - V)\, k_2\, \omega - V\, \omega \right\} ,$$

$$Y = M_o \left\{ (\dot{V} - \dot{v})\, k_2 + \dot{V} - (u - U)\, k_1\, \omega + U\, \omega \right\} ,$$

$$N = - I_o\, k'\, \dot{\omega} - M_o (k_2 - k_1)(u - U)(v - V) .$$

These are the equations of the hydrodynamic reactions on a body moving in a perfect fluid which itself has linear motion at a great distance. It is noted that for $U = V = \dot{U} = \dot{V} = 0$ they reduce to equations given in the several texts for the motion of a body in a fluid at rest at infinity.

It is remembered that these reactions are those that exist in the inertial system in which the linear motions of the body and fluid are measured, and that they are directed along the instantaneous directions of body axes.

The velocity of the fluid at a distance will now be resolved along axes x_o, y_o fixed in space. It is necessary to define the angular orientation of the body with respect to the x_o, y_o axes. This quantity shall be

taken as the angle of yaw of the x body axis from the fixed direction of the x_o axis. The symbol β will be used, although it is usually reserved for the true angle of yaw of the x axis from the direction of the total linear velocity of the body.

$$U = U_o \cos\beta + V_o \sin\beta$$

$$V = -U_o \sin\beta + V_o \cos\beta$$

$$X = M_o \left\{ (\dot{U} - \dot{u})\, k_1 + (v - V)\, k_2\, \omega + \dot{U}_o \cos\beta + \dot{V}_o \sin\beta \right\}$$

$$Y = M_o \left\{ (\dot{V} - \dot{v})\, k_2 - (u - U)\, k_1\, \omega - \dot{U}_o \sin\beta + \dot{V}_o \cos\beta \right\}$$

$$N = - I_o\, k'\, \dot{\omega} - M_o\, (k_2 - k_1)\, (u - U)\, (v - V) .$$

The effect of the motion of the fluid at infinity is clearly seen from this form of the equations. For the case of zero fluid acceleration at a great distance for the two-dimensional motion of a prolate ellipsoid, the hydrodynamic reactions on the body are functions of the relative motion of the body and fluid. These reactions may be measured in any inertial system in which the velocity of the fluid at a great distance is constant.

DISTRIBUTION LIST

CONTRACT N6onr-24435, PROJECT NR 062-124

Chief of Naval Research
Department of the Navy
Washington 25, D. C.
Attn: Code 438 (2)

Commanding Officer
Office of Naval Research
Branch Office
The John Crerar Library Bldg.
86 East Randolph Street
Chicago 1, Illinois (1)

Commanding Officer
Office of Naval Research
Branch Office
346 Broadway
New York 13, New York (1)

Commanding Officer
Office of Naval Research
Branch Office
1030 East Green Street
Pasadena 1, California (2)

Commanding Officer
Office of Naval Research
Branch Office
1000 Geary Street
San Francisco 24, Calif. (1)

Commanding Officer
Office of Naval Research
Branch Office
Navy No. 100, Fleet Post Office
New York, N. Y. (2)

Director
Naval Research Laboratory
Washington 25, D. C.
Attn: Code 2021 (6)

Commanding Officer
Naval Ordnance Laboratory
White Oak
Silver Spring, Maryland (1)

Chief, Bureau of Aeronautics
Department of the Navy
Washington 25, D. C.
Attn: Research Division (1)

Chief, Bureau of Ordnance
Department of the Navy
Washington 25, D. C.
Attn: Code Re3d (1)
Code Re6a (1)
Research and Development Div. (1)

Chief, Bureau of Ships
Department of the Navy
Washington 25, D. C.
Attn: Research Division (1)

Commanding Officer and Director
David Taylor Model Basin
Washington 7, D. C.
Attn: Hydrodynamics Division (1)
Technical Library (1)

Commander
Naval Ordnance Test Station
Inyokern, China Lake,
California
Attn: Code 5507 (1)

Commander
Naval Ordnance Test Station
3202 E. Foothill Blvd.,
Pasadena, California
Attn: Code P5507 (1)

Commander
Submarine Development Group TWO
Box 70
U. S. Naval Submarine Base
New London, Connecticut (1)

Office of Ordnance Research
Department of the Army
Washington 25, D. C. (1)

Director of Research
National Advisory Committee
for Aeronautics
1724 F Street, N. W.
Washington 25, D. C. (1)

Director
National Bureau of Standards
National Hydraulics Laboratory
Washington 25, D. C. (1)

DISTRIBUTION LIST

CONTRACT N6onr-24435, PROJECT NR 062-124

(Continued)

Documents Service Center
Armed Service Technical Information
Agency
Knott Building
Dayton 2, Ohio (5)

Mr. C. A. Gongwer
Aerojet General Corporation
332 N. Irwindale Road
Azusa, California (1)

Dr. A. T. Ippen
Hydrodynamics Laboratory
Massachusetts Institute of Technology
Cambridge 39, Mass. (1)

Dr. J. M. Robertson
Ordnance Research Laboratory
Pennsylvania State College
State College, Pennsylvania (1)

Dr. Hunter Rouse, Director
Iowa Institute of Hydraulic Research
State University of Iowa
Iowa City, Iowa (1)

Stevens Institute of Technology
Experimental Towing Tank
711 Hudson Street
Hoboken, New Jersey (1)

Dr. L. G. Straub
St. Anthony Falls Hydraulic
Laboratory
University of Minnesota
Minneapolis 14, Minnesota (1)

Technical Librarian,
AVCO Manufacturing Corporation
2385 Revere Beach Parkway
Everett 49, Massachusetts (1)